

Received September 23, 2019, accepted October 19, 2019, date of publication October 23, 2019, date of current version November 4, 2019.

Digital Object Identifier 10.1109/ACCESS.2019.2949131

# Time-to-Collision-Based Awareness and Congestion Control for Vehicular Communications

JUAN AZNAR-POVEDA<sup>ID</sup>, ESTEBAN EGEA-LOPEZ<sup>ID</sup>, ANTONIO-JAVIER GARCIA-SANCHEZ<sup>ID</sup>, AND PABLO PAVON-MARIÑO<sup>ID</sup>

Department of Information and Communications Technologies, Universidad Politécnica de Cartagena, Cartagena 30202, Spain

Corresponding author: Esteban Egea-Lopez (esteban.egea@upct.es)

This work was supported in part by Spanish MECD/AEI/FEDER under Grant TEC2016-76465-C2-1-R, in part by Spanish MINECO/AEI/FEDER under Grant TEC2017-84423-C3-2-P (ONOFRE-2), in part by e-DIVITA under Grant 20509/PDC/18 (Proof of Concept, 2018), and in part by ATENTO Projects under Grant 20889/PI/18 (Fundación Seneca, Región de Murcia). The work of J. Aznar-Poveda was supported by the MECD under Grant BES-2017-081061.

**ABSTRACT** Vehicular wireless communications require both congestion control to guarantee the availability of a fraction of the bandwidth for safety-related event-driven messages in emergency cases, and awareness control to adapt the beaconing activity to the application needs and surrounding traffic situation. Most current approaches either ignore the traffic situation and only adapt the beaconing rate to the channel congestion state or override the congestion control limits, leading to questionable results in both cases. In this paper, we conceive and validate a novel approach, combining both aspects. Based on distributed Network Utility Maximization (NUM), our algorithm satisfies the constraints on channel availability, whereas the safety of the surrounding traffic situation is captured with a time-to-collision metric, used to assign priorities in the optimal allocation problem. The performance of the proposed approach is validated and compared to other popular algorithms. Results show that our proposal automatically anticipates a potential increase in rate due to a critical safety situation, but does not interfere with the reserved bandwidth for safety applications.

**INDEX TERMS** Awareness control, beaconing rate control, congestion control, time-to-collision, vehicular communications.

## I. INTRODUCTION

Connected vehicles extend the capabilities of multiple advanced driver-assistance systems and automated vehicles by enabling the possibility of performing cooperative actions, such as Cooperative Automated Driving (CAD) or increasing the awareness of a vehicle's sensor systems [1]. CAD can improve safety and efficiency by introducing Cooperative Adaptive Cruise Control (CACC) applications [2], including not only platoon driving, but also cooperative collision avoidance [3], among others.

Cooperative inter-vehicular applications usually rely on the exchange of broadcast single-hop status messages (*beacons*) among vehicles on a single control channel, which provides detailed information about vehicle position, speed, heading, acceleration, curvature, and other data of interest [4]. Beacons, called Cooperative Awareness Messages (CAM)

The associate editor coordinating the review of this manuscript and approving it for publication was Qingchun Chen<sup>ID</sup>.

in European standards and Basic Safety Messages (BSM) in the US standard, are transmitted periodically at a certain *beaconing rate*. The aggregated load on the wireless channel due to periodic beacons can rise to a point where it can limit or prevent the transmission of other crucial messages, which is called *channel congestion due to beaconing activity*. Even though this problem has been previously analyzed by different related proposals [5]–[10], some aspects deserve further consideration.

In this regard, there are two different approaches to the control problem: pure *congestion control*, (CC) and *awareness control*, (AC) [11]. Congestion control usually refers to the mechanisms used to keep the channel load at the desired level, irrespective of the needs of the applications on top of the service. In contrast, awareness control usually refers to the mechanisms employed to satisfy *some application requirements*. To the best of our knowledge, although there is no widely accepted common definition for awareness, it is usually related to the notion that the beaconing rate

should adapt to traffic or vehicle situations [12], especially as regards safety [13], and not only to the channel load. Although related, both approaches call for different solutions, with different results, requirements, and inputs.

To illustrate the differences between both approaches, consider the following situations from the adopted solutions in the standards: purely CC, such as LIMERIC [5], updates the beaconing rate *only* according to the locally measured state of the wireless channel. This immediately raises the question of what to do when the same channel is shared by vehicles with different traffic states, such as a free flow of high-speed vehicles in one direction of a highway, and a traffic jam in the opposite direction. An AC oriented solution is to let vehicles generate beacons according to *their own* dynamics, as specified in [4], and proposed in [7], [10], [14], [15] among others. Which in turn raises more questions. First, should this mechanism always be limited by the CC or should it be able to violate the CC-imposed limits on bandwidth usage in some circumstances? In the former case, the previous problem persists, while in the latter case, the effectiveness of the CC has to be evaluated, as well as potential interference with other services, such as Decentralized Environmental Notification (DEN), which requires the access network not to be in a congested state. Second, if the CC only limits but does not trigger beacon generation, the channel is underused, at least with the generation rules of [4], so why not use all the available resources if the quality of services of applications benefits from a higher rate? Moreover, non-reactive CC mechanisms [5], [6] are usually designed to *drive the load* to a desired point. If they are just used to limit the rate, the results and performance may not be as designed. Reactive controls, such as the one in the standard [16], on the other hand, suffer from instabilities [8]. Third, if the vehicle does not evaluate the safety of its surrounding traffic situation but generates beacons only according to its own dynamics, some particular situations yield questionable results. For instance, a vehicle stopped in the middle of a highway may be a danger, but current beacon generation rules [4] force it to transmit at the minimum beaconing rate. This particular example is actually mentioned in the standards for various collision risk warnings [17]–[19].

Current European standards specify the separation of beacon generation and congestion control [4]; the latter strictly limits the rate, reproducing the aforementioned concerns. The beacon generation rules only depend on the vehicle's own dynamics, which results in a type of limited awareness control, as we have pointed out. The underlying issue seems to be how to integrate congestion and awareness control, including beacon generation, into a more coherent framework with more clearly defined goals. Additional desirable features of the procedure are that it is distributed as well as providing provable fairness, stability, and convergence.

In this paper, we discuss these issues and propose a novel awareness control mechanism that complements the pure congestion control of our previous FABRIC protocol [6], by taking advantage of the algorithm's capability to shape

the resulting allocation using fairness and priority parameters. Our goals are, first of all, that the surrounding traffic situation and neighboring dynamics be taken into the account by the awareness control. To this purpose, vehicles evaluate the safety of the traffic situation by computing the Time-To-Collision (TTC) with their known neighbors with a simple but generic procedure, and the result is used to set the priority parameter, which provides *weighted fairness*. Based on a Network Utility Maximization (NUM) problem with constraints, it assigns differentiated rates but enforces a Maximum Beaconing Load (MBL) constraint. So, in this way, we achieve our second goal, which is to effectively integrate awareness control with congestion control. Road safety signaling services, such as DEN, maintain a reserved bandwidth and eliminate the potential interference. Finally, our approach also provides guarantees of convergence to a fair allocation solution, supported by the rigorous developments of the NUM theory [6].

In Sect. II, we discuss related work. Then, a brief review of our previous work, as well as an illustration of its capabilities is provided in Sect. III. We describe our proposal in Sect. IV, and simulate it in Sect. V, providing a comparison with other algorithms, and discussing the obtained results. Finally, Sect. VI summarizes the main conclusions.

## II. RELATED WORK

ETSI standards define, as one of the basic network access technologies, a 10 MHz control channel for vehicular communications at 5.9 GHz [20], the ITS-G5 radio channel. Transmissions over this access network are broadcast in nature and use CSMA-based medium access control (MAC), with no acknowledgment or retransmission. The ETSI Cooperative Awareness Service (CAS) [4] requires periodic beaconing over one-hop broadcast communications to support cooperative awareness by disseminating status and environmental information to vehicles on the control channel [4]. In addition, ETSI standards specify the Cross-Layer Decentralized Congestion Control (DCC) Management Entity [21], whose goal is to avoid overloading the ITS-G5 radio channel.

The algorithm specified by European standards, which we call here CAM-DCC, is the combined operation of two procedures: the vehicle dynamics dependent CAM generation rules, specified in [4], and the simple reactive congestion control algorithm suggested in [16]. More specifically, CAM-DCC measures the absolute difference between a current heading, position, and speed, and those included in the previously transmitted CAM. If the time elapsed since the last generation and one of these conditions overcome pre-defined thresholds, a new CAM will be generated. This procedure presents two drawbacks: i) a lack of clear motivation for the triggering rules, and ii) a CAM synchronization problem for cooperative maneuvers that seriously degrades its performance, as discussed in [9]. Moreover, a lack of responsiveness for faster vehicles is found in [22], which results in an absence of fairness. The second part, the reactive congestion control, is based on a finite state machine which

results in oscillations, as reported in [8]. In contrast, most of the available proposals do not separate CAM generation from congestion control.

To limit the load on the channel, several transmission parameters can be controlled, such as the beaconing rate, transmission power [23], data rate and joint combinations of them [15], [24]. Given the broad scope of solutions and to keep the review focused, we first discuss relevant beaconing-rate CC proposals and later AC proposals which in some cases incorporate joint control of other parameters. In the category of rate-based controls, LIMERIC [5] is a distributed and adaptive linear rate-control algorithm in which each vehicle linearly updates its own rate depending on the total load, which is driven towards a required goal. This a pure CC mechanism, since only the channel load is used to update the rates, whereas vehicle dynamics, application requirements, and traffic situations are completely ignored. PULSAR [25] is another pure rate control algorithm that uses Additive Increase Multiplicative Decrease (AIMD) with feedback from 2-hop neighbors. The convergence of LIMERIC is only proved when all the vehicles are in range of each other; not for multi-hop scenarios. Therefore, authors of LIMERIC propose some modifications [26] to use the rate adaptation employed in LIMERIC in multi-hop scenarios by combining it with the PULSAR proposal [8]. The outcome, however, of this combination is that all the vehicles sharing a link converge to the rate of the most congested link, which unnecessarily decreases the rate of some vehicles, even though they do not measure channel congestion. A more detailed discussion and examples of this problem can be found in our previous work [6].

Regarding awareness control and the application requirements that determine the beaconing rate, different alternatives can be found in the literature. There is a set of proposals whose aim is to adjust the rate in order to minimize the position tracking error with respect to other vehicles, such as [27] and [7], which is actually the mechanism for the US DCC standard [28], or EMBARC [14], a variation of LIMERIC, which integrates the tracking error algorithm of [7]. Other proposals assess the estimated risk of some traffic situations, especially intersections, such as [13], where an estimated collision probability for intersections triggers the transmission rate adjustment. CAM-DCC can be considered another proposal for awareness control, as it adapts the beaconing rate to current vehicle dynamics. Several works define [29], [30] some risk metrics based on the vehicle dynamics and traffic situation, similar to our TTC metric, but with less general models. Finally, there are some application-agnostic proposals, such as INTERN [12], which directly assigns the rate that an application demands and then equally shares the excess capacity.

Regarding the way AC is integrated with CC one can find approaches that directly *override or ignore* congestion control [13], [27], [30], and others that *integrate* congestion control in some way [4], [7], [10], [12], [14], [15], [29]. Among the proposals that actually integrate CC and AC

effectively, NORAC [10] is a rate and awareness distributed control based on non-cooperative game theory, whose more relevant feature is that it does not require the exchange of control information. Each vehicle can independently use a utility parameter and a price parameter to adjust the behavior of the algorithm. The utility parameter is used to assign a rate to a vehicle proportional to its requirements, which is the way to provide priority or *weighted fairness* and, consequently, AC when it is demanded by some application. In this sense, it is quite similar to our proposal, where we also use a per-vehicle parameter to provide weighted fairness, as described below. However, in contrast to our proposal, constraints are not considered in NORAC and so an MBL cannot be explicitly set. The resulting channel load and shape of the allocation is determined by the combinations of price and utility parameters and no systematic procedure to select them is provided. These same limitations apply also to BFPC [15], a recent proposal, which incorporates joint power control to NORAC. ABC [29] also integrates AC and CC in the context of a TDMA-based protocol. In this case, the potential risk of a rear-end collision is incorporated in an optimal resource allocation problem in order to assign more resources to more dangerous vehicles. In our proposal, we also prioritize the rate vehicles involved in potentially riskier situations, but with a more general kinematic model, not limited to rear-end collisions, and which integrates seamlessly in our algorithm, without the computational and communication overhead of ABC.

The problem of beaconing rate control for vehicular networks has been modeled as a NUM problem [31], [32] in our previous work [6]. The different fairness notions that can be induced on rate allocations and its fast convergence are shown in multi-hop and dynamic scenarios. The NUM approach has also been applied to power control [23], and joint power and rate control [24]. For a different problem, in [33], the probability of transmission under a slotted  $p$ -persistent vehicular broadcast medium access is formulated as a NUM problem, which takes the driving context into account to prioritize packets.

A further discussion about the limitations of these approaches is deferred to Sect. IV-A, where we link it to our proposal.

### III. BACKGROUND

In a previous paper [6], we derived an optimal congestion control algorithm for the beaconing rate based on a NUM approach. The key advantage of this approach is that it allows us to design a broad family of decentralized and simple algorithms with proven convergence guarantees to a fair allocation solution. That is, the rate allocation is guaranteed (i) to be optimal, (ii) to comply with the constraints, and (iii) to enforce a particular fairness notion. We remark that this approach leads to a *family of algorithms* because different results are achieved depending on the values of a couple of parameters, which will be described later in this section. In our previous paper, we did not discuss how to select these parameters, but their appropriate choice provides

further enhancements to the algorithm. Before we discuss this, we briefly review the procedure and provide the algorithm for the sake of completeness.

Let  $V$  be a set of vehicles in a vehicular network. Each vehicle  $v \in V$  transmits beacons at a rate  $r_v$  beacons/sec,  $r_v \in [R_v^{min}, R_v^{max}]$ , with a constant transmission power. Beacons are broadcast and received by surrounding neighbors within the reception range. Let  $n(v)$  denote the set of neighbor vehicles of  $v$ , which also includes  $v$ . Let us note that each vehicle has its own set of neighbors, i.e., not all vehicles are in range of each other. The total rate received by each vehicle is the sum of the rates in its set of neighbors and we are interested in limiting this amount to a maximum  $C$  (beacons/s) to avoid channel congestion. Let  $U_v(r_v)$  be a utility function,  $\mathbf{R} \rightarrow \mathbf{R}$ .

With our approach, the beaconing rate allocation is the solution to the optimization problem (1) given by:

$$\max_{r_v} \sum_v U_v(r_v) \quad \text{subject to:} \quad (1a)$$

$$\sum_{v' \in n(v)} r_{v'} \leq C \quad \forall v \in V \quad (1b)$$

$$R_v^{min} \leq r_v \leq R_v^{max} \quad \forall v \in V \quad (1c)$$

Problem (1) achieves two goals: (i) to control congestion, while (ii) maximizing the allocated rates in a controllable and fair way. Congestion control is enforced by constraints (1b), which means that the beaconing load of a given vehicle, given by the rates generated by the neighboring vehicles, plus its own must be below  $C$ , which is a fraction of the available channel capacity. Constraints (1c) force the vehicle rate to be within a minimum ( $R_v^{min}$ ) and maximum ( $R_v^{max}$ ) range as required by the standards. The objective function to be maximized is the sum of the utility  $U_v(r_v)$  of each vehicle, which is a function of the rate  $r_v$  allocated to it. Therefore, *the shape of the utility function determines how the rates are maximized.*

In fact, the link to the enforced fairness notion comes from an appropriate selection of the utility function: the use of the so called  $(\alpha, \omega)$  utility functions, shown in equation (2), guarantees that the solution to problem (1) is also *fair* according to well-defined fairness notions, as shown in [32].

$$U_v(r_v) = \begin{cases} \omega_v r_v, & \text{if } \alpha = 0 \\ \omega_v \log r_v, & \text{if } \alpha = 1 \\ \omega_v \frac{r_v^{1-\alpha}}{1-\alpha}, & \text{if } \alpha > 1 \end{cases} \quad (2)$$

Let us now discuss the selection of the parameters of problem (1) when we insert the  $(\alpha, \omega)$  utility functions:

- The Maximum Beaconing Load (MBL), given by  $C$ , is usually set at a fraction of the available channel capacity, which depends in turn on the transmission rate used. A transmission rate of 6 Mbps is usually selected because of its robustness, though this has recently been questioned [34]. A 60% of the whole available capacity is usually selected because it is the optimum beaconing

load concerning several metrics [7], [35]. The remaining 40% of the available capacity is left unused to guarantee the delivery of event-driven messages in emergency cases.

- The minimum  $R_v^{min}$  and maximum  $R_v^{max}$  beaconing rates are set by the standards [4], at 1 and 10 beacons/s respectively. However, with our approach, each vehicle may independently set its minimum and maximum rates if necessary, to guarantee minimum application reliability, and the algorithm will allocate the remaining rates to meet the constraints.
- The *fairness parameter*,  $\alpha$ , allows us to adjust the notion of fairness. In particular,  $\alpha = 0$  maximizes the throughput but may result in arbitrarily unfair solutions where some nodes are granted all the resources and others, none. With  $\alpha = 1$ , proportional fairness, as defined by Kelly [31], is achieved. Finally, as  $\alpha \rightarrow \infty$ , the allocation tends to max-min fairness.
- The *priority parameter*,  $\omega_v$ , is used to prioritize the rate allocated to particular  $v$  vehicles; that is, to achieve *weighted fairness*.

The above optimization problem is solved via its dual problem in a distributed way including a gradient-descent based algorithm [6], shown in Algorithm 1.

---

**Algorithm 1** FABRIC [6]

---

- 1 Set initial vehicle prices  $\pi_v^0$  and rates  $r_v^0$ .
  - 2 **foreach** interval  $k$  **do**
  - 3     Each vehicle  $v$  receives the prices of neighbor vehicles  $\pi_{v'}, v' \in n(v)$
  - 4     At the end of interval  $k$ , each vehicle updates its rate  $r_v^k(\pi)$  according to:
  - 5      $r_v^{k+1}(\pi) = \left[ \left( \frac{\omega_v}{\sum_{v' \in n(v)} \pi_{v'}} \right)^{\frac{1}{\alpha}} \right]_{R_v^{min}}^{R_v^{max}}$
  - 6     Finally, each vehicle computes its new price:
  - 7      $\pi_v^{k+1} = \left[ \pi_v^k - \beta \left( C - \sum_{v' \in n(v)} r_{v'}^k \right) \right]_0$
  - 8 **end**
- 

In [6], the evaluation of the influence of  $\omega$  was left as future work, setting  $\omega_v = 1$  for all vehicles. Also, it was remarked that there is no consensus about which particular value of  $\alpha$  is best suited for vehicular networks. The criteria for selecting a particular fairness notion are application dependent. We demonstrated and discussed its effects with examples, which, in our opinion, tend to favor proportional fairness versus max-min fairness.

In this way, in this paper, we return to the question of parameter selection to achieve the full potential of the algorithm and the best way to tune it to vehicular network requirements.

Before putting forward our proposal, in the next section, we evaluate the influence of the parameters to determine its sensitivity and potential to determine the results according to a particular goal.

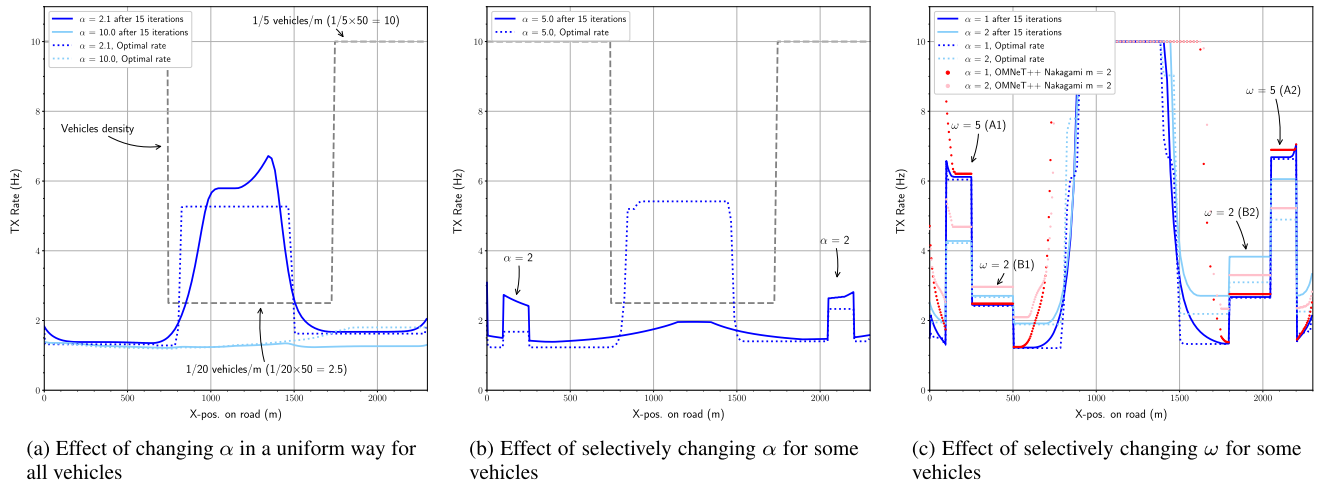


**FIGURE 1.** Exact optimal allocation and FABRIC with different values of fairness ( $\alpha$ ) and priority ( $\omega$ ) parameters for selected vehicles after 15 iterations. Vehicle density (vehicles/m) marked in a dotted gray line and scaled by 50 to match the beacon rate axis.

**A. INFLUENCE OF PARAMETERS ON THE ALGORITHM**

We have evaluated Algorithm 1 (FABRIC) of [6], for different values of  $\alpha$  and  $\omega$ . In this evaluation, neither propagation nor additional protocol layers are considered, as our goal at this point is to characterize only the influence of each parameter without distortions due to other effects. The behavior of the algorithm with realistic settings is shown in the results section. Besides, the *exact optimal allocation* has been computed using a numerical solver implemented with the Java Optimization Modeler (JOM) library. The exact solution as well as the results of FABRIC after 15 iterations, starting from the maximum rate, are plotted in Fig. 1. A simple highway scenario has been recreated, consisting of 310 vehicles evenly spaced in the  $x$  axis every 5 m (high-density region), except those vehicles between numbers 150 and 200, which are spaced every 20 m (low-density region). In the following explanation, we always consider the  $x$  axis to be the longitudinal axis of the highway, and the  $y$  axis, the traversal axis. The MBL has been set to  $C = 200$  beacons/s and a deterministic transmission range of 400 m is assumed.

In the first test, we set an equal weight,  $\omega = 1$ , for all the vehicles and vary the parameter  $\alpha$ . As can be seen in Fig. 1a, the effect of increasing  $\alpha$  is to equalize the allocated rates, as expected. As  $\alpha$  grows, the allocation tends to a max-min solution where the rates are determined by the bottleneck links, that is, *the congested channel regions force vehicles in not congested channel areas to reduce their rates*. These are actually the results obtained with other proposals, such as LIMERIC+PULSAR, as was also shown in [6]. We do not think this is generally desirable, because the rate of vehicles in areas with a not congested channel is unnecessarily reduced, even though there is available channel capacity; that is, the load is below the MBL.

In the second test, we examine whether it is useful to prioritize the beaconing rates by selectively changing the  $\alpha$  parameter for some vehicles in the network. In Fig. 1b,

we show the results of setting  $\alpha = 2$  for vehicles 20 to 50 and 260 to 290, while leaving  $\alpha = 5$  for the rest of the vehicles, and keeping  $\omega = 1$  for all of them. The results show that it is actually possible to prioritize those vehicles, but *there is no clear mapping between the values of  $\alpha$  and the allocated rates*. Moreover, the use of a high value of  $\alpha$  is detrimental to the convergence and we would need more iterations to achieve a better match. Let us also note that the differences between the rates obtained in each cluster of vehicles (20-50 and 260-290) are due to the different number of neighboring vehicles located in their surrounding area, since, as can be observed in the figures, the vehicle density is not symmetric.

Finally, we set the parameters in the natural way; that is, we use  $\omega$  to prioritize some vehicles and  $\alpha$  to induce a global fairness notion. We have set  $\omega = 5$  for vehicles 20 to 50 (group A1) and 260 to 290 (group A2),  $\omega = 2$  for vehicles 50 to 100 (group B1) and 210 to 260 (group B2), and  $\omega = 1$  for the remaining ones. In addition, we have plotted the results for  $\alpha = 1$  (proportional fairness) and  $\alpha = 2$ . The MBL has been increased to  $C = 400$  beacons/s to give more leeway to the allocation of the rates. As can be seen in Fig. 1c, if there is enough capacity, *with proportional fairness, the allocated rates are proportional to the  $\omega$  ratios*, as expected. For instance, for vehicles in A1 and B1, we have  $\frac{r_{A1}}{r_{B1}} = \frac{6.09}{2.437} = \frac{\omega_{A1}}{\omega_{B1}} = \frac{5}{2}$  and the ratio of A1 for the rest of the vehicles in the high density area  $\frac{r_{A1}}{r} = \frac{6.09}{1.219} = \frac{\omega_{A1}}{\omega} = \frac{5}{1}$ . Similarly,  $\frac{r_{B1}}{r} = \frac{\omega_{B1}}{\omega} = \frac{2}{1}$ . Moreover, in the low density area, even though here  $\omega = 1$ , the vehicles set the maximum rate because there is available capacity. Let us note that this behavior is general; not dependent on this particular scenario. From eq. (7), later, it follows that the ratios of rates of vehicles  $i$  and  $j$ , measuring the same congested channel state, are given by  $\omega_i^{\frac{1}{\alpha}} / \omega_j^{\frac{1}{\alpha}}$ . These results suggest that fine tuning of the allocated rates can be achieved by appropriately setting the  $\omega$

parameter, while the  $\alpha$  parameters allow us to smooth out the differences. Since the algorithm adapts to these parameters dynamically, we can use them to support further application requirements. In other words, fairness and congestion control are automatically fulfilled by directly applying the algorithm with equal parameter settings; but by selectively assigning values to the parameters, weighted fairness and therefore awareness control can be achieved.

To illustrate the behavior in a more realistic scenario, we have simulated it with OMNeT++ [36], setting a Nakagami-m propagation model and a IEEE 802.11 MAC. The results after 15 iterations are also plotted in Fig. 1c. It can be seen that even when we include fading and collisions, the results are reasonably close to the values of the ideal setting. They cannot be equal because the sharp differences in the ideal case are a consequence of the deterministic number of neighbors of the vehicles, whereas fading smoothes the shape of the allocation.

Let us conclude with a brief discussion on the convergence of the algorithm, since both  $\alpha$  and  $\omega$  affect in it [6]. We consider the basic synchronous algorithm, due to that their influence is more clearly seen, while the conclusions apply qualitatively to other variants. According to [37], the convergence of the gradient descent depends on the value of the gradient step  $\beta$  (line 7 in Algorithm 1) and, in the considered case, it must satisfy the following inequality (3):

$$\beta < \frac{2}{\bar{L}\bar{N}\bar{c}} \quad (3)$$

where  $\bar{L}$  is the length of longest path (links or hops in our context) used by the sources ( $\bar{L} = 1$ ),  $\bar{N}$  the number of vehicles that share the most congested link, and  $\bar{c}$  is a bound of the second derivative with respect to the beaconing rate of the utility function [37]:

$$-\frac{d^2U(r)}{dr^2} \geq \frac{1}{\bar{c}} \quad (4)$$

By introducing the utility function (2) in equations (4) and (3) and considering the maximum rate, we have:

$$\beta < \frac{2\alpha\omega}{R_{max}^{\alpha+1}\bar{N}} \quad (5)$$

This leads to the following guidelines: (i) The higher the  $\alpha$  parameter is, the slower the convergence since we are forced to use a smaller gradient step  $\beta$ . And (ii), by the opposite reason, a greater  $\omega$  parameter helps to improve the convergence. We will come back to these parameters in Sect. IV-D, when we describe our proposal more in detail.

Now, the question is how to set these parameters to effectively enforce some notion of awareness control while maintaining a high convergence speed. From the previous discussion and results we favor the use of a low  $\alpha$ : A value of 1 allows us to obtain proportional fairness and quick convergence, but values around 2 may be used to get more balanced allocations without degrading convergence.

As for the awareness control via weighted fairness including the  $\omega$  parameter, in the next section, we will discuss several approaches and propose our own.

#### IV. PROPOSED ALGORITHM

In this section, we first discuss the limitations of other awareness and congestion control algorithms. Then, based on the conclusions we introduce our proposal.

##### A. LIMITATIONS OF CURRENT PROPOSALS

In Sect. I and II, we pointed out that the main problem with pure CC approaches is that they ignore the traffic situation of the vehicle and only use channel information, with additional problems if the beacon generation is separated from the congestion control. Regarding AC, some of them integrate CC in some way, but most of them ignore or override it. However, care should be taken when overriding beaconing congestion control. One of the goals of congestion control is to facilitate the operation of event-driven messages, such as those of DEN in ETSI standards, by guaranteeing that a given fraction of the channel capacity is available for this service. The intended functionality of each service, CAS and DEN, should be kept separate in our opinion. For instance, using estimated collision probability at an intersection [13] seems more suitable for a road hazard signaling (RHS) application that uses periodic event-driven messages, as suggested in [17, Annex B], rather than CAM messages. And by not actually enforcing the MBL, some proposals *may interfere* with the DEN service even though they take congestion control into account in some way. This is the case of INTERN, whose authors recognize the difficulties of ubiquitously satisfying application requirements and discuss feasible regions where this is possible. The issue, then, is how to avoid those regions, which again points to a clearer mapping between the CAS or DEN service and the nature of the application. In fact, they have recently proposed a coordination methodology described in [38].

Many AC proposals aim to adapt the rate to minimize the position tracking error with respect to other vehicles, such as [27] and [7], which is the mechanism for the US DCC standard [28], or EMBARC [14], a variation of LIMERIC which integrates the tracking error algorithm of [7]. The proposals that use tracking error to trigger new beacon generations [7], [14], [27], essentially *adapt the beaconing rate to their own vehicle dynamics*. Therefore, CAM-DCC also falls into this category. In the absence of variations, few or even no additional beacons are generated. Our main concern with this approach is that *it ignores the surrounding traffic situation*. The previously discussed example of a highway with a traffic jam in one direction, resulting in a congested channel, and a free-flow condition in the opposite direction with high-speed vehicles, applies here. The vehicles in free-flow are forced to decrease their rates due to the congested channel and, even with error tracking control, if they do not change their speed or heading significantly, no additional beacons are generated. Some others, such as NORAC [10] and explicitly BFPC [15], address the problem by setting the rates

proportional to the speed, but again they only consider the dynamics of each vehicle, in particular, the speed, not the surrounding traffic, which, for instance, leads to that a single stopped vehicle in the middle of a highway reduces the rate instead of increasing it. It must be said that both NORAC and BFPC only introduce the speed as an example of a potentially suitable weight function and that others, such as our own TTC proposal, might be used with these algorithms.

In fact, the single stopped vehicle example is used in ETSI standards for safety-related applications, such as RHS [17], ICRW [18], LCRW [19], when discussing CAM adaptation, saying that, in some situations, the solutions based on “highly dynamic data evolutions”, that is, the dynamics of the ego vehicle *may* not be suitable and adjustment by the corresponding safety application, “based on the perceived criticality of the traffic safety situation around the vehicle [...], would be more meaningful” [17, Annex F]. In other words, the traffic situation should be taken into account. From our point of view, even though some recent proposals address these issues, some aspects are missing and potentially more satisfactory solutions can be still explored.

**B. TIME-TO-COLLISION CONGESTION CONTROL (TTCC)**

We propose a type of awareness control that complements the pure congestion control of [6] by taking advantage of the algorithm’s capability to shape the resulting allocation via fairness and priority parameters. The considerations of the previous section suggest the following goals:

- The awareness control should be fully integrated with the congestion control and comply with the MBL constraint. This way, safety services are guaranteed a reserved bandwidth. If this is not feasible because of application requirements, one should consider whether the application should use the CAS as the main dissemination service.
- The awareness control should take the surrounding traffic situation and neighboring dynamics into account.

A usual metric to assess the criticality of a safety situation is Time-to-Collision (TTC), as discussed in ETSI standards [17]–[19] and other works [39]. We use it as the basis for prioritizing beaconing rates. To compute it, we use simple kinetics, but formulated in a general vector form, which can be applied to most situations without assuming limiting simplified models [29], [30], such as one-dimensional (1D) models or just ahead-vehicle tracking. Let us assume a three-dimensional (3D)<sup>1</sup> scenario, such as the scenario depicted in Figure 2. We represent each vehicle as a sphere of radius  $r_v$ , and its movement with three different vectors of acceleration, velocity, and position,  $\vec{A}$ ,  $\vec{V}$ , and  $\vec{P}$ , respectively.

Assume that TTC will be computed at regular intervals of time, which are short enough to presume that the acceleration in that interval will remain constant. In this case, we can ignore complex real-vehicle dynamics and use simple

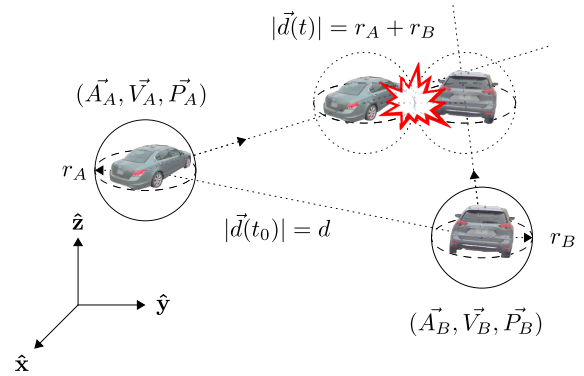


**FIGURE 2. Notation and scenario used to derive the time-to-collision (TTC) metric, used in this article.**

constant-acceleration kinetics as estimations of future vehicle position:  $\vec{P}(t) = \vec{P}_0 + \vec{V}t + \frac{1}{2}\vec{A}t^2$ .

A collision between two vehicles occurs at time  $t$  when their corresponding spheres overlap. To compute this, it is easier to use a relative formulation, where the  $R$  subscript denotes the difference between  $A$  and  $B$  vectors:  $\vec{S}_R = \vec{P}_A - \vec{P}_B$ ,  $\vec{V}_R = \vec{V}_A - \vec{V}_B$  and  $\vec{A}_R = \vec{A}_A - \vec{A}_B$ .

Therefore,  $d(t)$ , the distance between two vehicles at time  $t$  is  $\vec{d}(t) = \vec{S}_R + \vec{V}_R t + \frac{1}{2}\vec{A}_R t^2$ . And there is a collision when  $\vec{d}(t) \cdot \vec{d}(t) = |d(t)|^2 = |r_A + r_B|^2$ . For the sake of simpler notation, we set  $r_A + r_B = r$ , and expand the dot product to get the following 4th order polynomial equation in  $t$ , eq. (6), whose solution gives the TTC between the two vehicles involved:

$$\frac{1}{4}A_R^2 t^4 + \vec{V}_R \cdot \vec{A}_R t^3 + (\vec{S}_R \cdot \vec{A}_R + V_R^2) t^2 + 2t\vec{S}_R \cdot \vec{V}_R + (S_R^2 - r^2) = 0 \quad (6)$$

where each  $\vec{u} \cdot \vec{u} = |u|^2 = u^2$ . If a constant-speed model is used, a straightforward quadratic equation is obtained, but we prefer to include the acceleration information.

The outline of the algorithm is: A vehicle computes the  $TTC_v$  for all its known neighbors, using the data contained in the beacons received from them and using the inverse of the minimum one to set its priority  $\omega_v$  in the utility function of Problem (1), as will be described in Sect. IV-D later.

Let us first discuss some qualitative features of this approach:

- It is obvious that the quality of the computed TTC depends on the quality of the received data. Alternatives that take noise into account can be considered. Just as the *suspected tracking error* is used by [7], [14], [27], a suspected TTC error may be also used. However, we focus here on the basic approach.
- The sphere radius can be set as half of the vehicle length to get a conservative value. Real or average values can be used. Trucks, buses, and long vehicles can be represented by multiple spheres. In general, further adjustments can be made to tune the procedure, but let us highlight how this concept aligns well with the notion of the *dynamic safety shield* mentioned in the ETSI safety

<sup>1</sup>A two-dimensional (2D) scenario is enough in most practical situations. The vector equations are the same in any number of dimensions.

standards [17]–[19], which set a vehicle in a state of increased alert when it detects that a neighbor is within a TTC threshold.

- Let us remark that our scheme aids, but does not overlap the DEN functionality. As TTCs decrease, our proposal increases the beaconing rate of potentially involved vehicles, which is absorbed by non-involved ones in advance. If a critical safety situation eventually occurs, the congestion control is overridden, if necessary, from the DEN. Therefore, this algorithm *automatically anticipates a potential increase in rate by the DEN due to a critical safety situation* as discussed in standards [17]–[19]. But only up to a point, since the MBL constraint is satisfied so it does not interfere with the reserved bandwidth, which is entirely available for the safety signaling application.

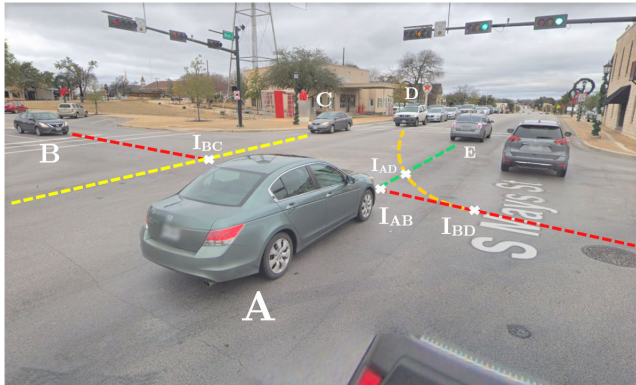


FIGURE 3. Intersection of 100 S may's St and main St, Round rock, Austin, Texas, USA. Image captured from google maps street view.

C. ILLUSTRATION OF TTC

Figure 3 shows a real situation which illustrates the need to consider the surrounding traffic situation globally. A vehicle  $i$  will compute a different  $TTC_{ij}$  for each of its neighbors, which depends upon the particular state of movement of the neighbor. For example, for vehicle A,  $TTC_{AE}$  may be long or short, depending on whether E accelerates or brakes.  $TTC_{AC}$  is very long (or infinity) because there is no collision risk, but  $TTC_{AD}$  may be low because the acceleration of D sets it on a collision course. The TTC has been represented in Figure 4 as a function of the relative speed for different separation distances and accelerations in a 1D scenario.

As expected, TTC reflects the risk related to the different combinations of parameters well. When a real root for TTC does not exist, it means an absence of risk. A collision would occur later as the separating distance increases and earlier as it decreases. Similarly, sudden deceleration owing to abrupt braking implies short values of TTC, and light braking, longer values of TTC. Let us note that this metric correctly reflects the risk in cases that may seem dubious. For instance, a closely tailgating vehicle with a very low relative speed and acceleration actually has a long TTC. In fact, one

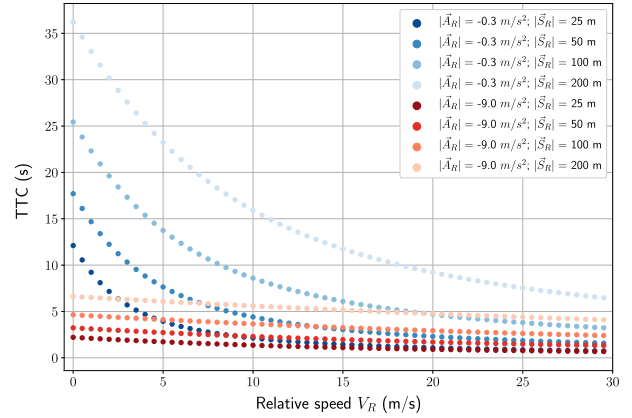


FIGURE 4. Time-to-collision evaluation between two vehicles for different accelerations, separation distances, and relative velocities  $V_R$ .

of the goals of CAD and cooperative platooning is to keep controlled relative speeds and accelerations to increase the capacity of the roads. Of course, in a normal situation tailgating vehicles would likely soon develop a non-zero relative speed or acceleration. But at that moment, the TTC would quickly decrease, reflecting again an increased risk.

D. TTCC ALGORITHM

Finally, here we describe the implementation of our TTCC algorithm. We have modified our previous algorithm by introducing the priority parameter in the optimization problem, determined by the computed minimum TTC, as we will discuss below. With this change, and checking the derivation [6, Sect. 4] mentioned in Section III, it directly follows that the optimal rate with the  $\omega$  parameter included is:

$$r_v^*(\pi) = \left[ \left( \frac{\omega_v}{\sum_{v' \in n(v)} \pi_{v'}} \right)^{\frac{1}{\alpha}} \right]_{R_v^{min}}^{R_v^{max}} \quad (7)$$

whereas the rest of the steps do not change. Therefore, the only necessary modification to our previous algorithm is the inclusion of the  $\omega$  parameter in eq. (7) and the selection of its value.

We now turn to the details of how *each vehicle v sets its  $\omega_v$* : a vehicle  $v$  computes the  $TTC_{vi}$  for all its known neighbors  $i$  from eq. (6). Only the real positive roots of eq. (6) give a valid TTC. The first approach is to use the inverse of the minimum valid TTC, found as the priority parameter  $\omega_v = \frac{1}{\min(TTC_{vi})}$ . But then, a solution with only imaginary roots means that no collision is possible with the given input: it would translate into a  $\omega_v = 0$ . In addition, TTC values can be arbitrarily large, which makes  $\omega_v$  tend to zero as well. We would prefer to assign  $\omega_v = 1$  to all the vehicles in the case that no minimum TTC is found, which more clearly conveys the idea that the vehicle does not need prioritization. We also introduce the  $\sigma$  parameter to rescale  $\omega$  to approximately match the scale of the rates and favors a quicker convergence as discussed below.



In addition, we introduce a speed term,  $S$ , to differentiate the speed among vehicles, so faster vehicles, even in absence of risk, are prioritized with respect to slower ones. Besides, it reflects the severity of a collision in case it may occur. This is done by means of the  $S$  term below:

$$S = 1 + \frac{v}{v_{MAX}} \quad (8)$$

which is the ratio of the vehicle speed to some maximum allowed speed  $v_{MAX}$ , plus one to guarantee that  $\omega$  is greater or equal to one. These parameters included in  $\omega$  have an influence on both the convergence of the algorithm and the ratios of the rates that we allocate to vehicles:

- First, to study the influence in the convergence of the algorithm, that is, its performance, we introduce the parameters in eq. (5) and get:

$$\beta < \frac{2\alpha}{R_{max}^{\alpha+1} \bar{N}} \left( \frac{\sigma}{TTC} + 1 + \frac{v}{v_{MAX}} \right) = \beta_0 \omega \quad (9)$$

We can observe how scaling the TTC with  $\sigma$  benefits the convergence by not forcing us to decrease the gradient step when the TTC is long. For the sake of clarity, we use a numerical example, and consider two TTCs, a short one,  $TTC_s = 0.5$  s, a long one,  $TTC_l = 50$  s, and  $v = 32$  m/s. Without scaling and  $S$ ,  $TTC_l$  would force us to decrease the step two orders of magnitude to ensure convergence,  $\beta < 2\beta_0 10^{-2}$ . With scaling of  $\sigma = 10$  we would only need to reduce one order of magnitude. But if we introduce the  $S$  term we achieve more stability, since when adding it to the scaled term, we make  $\omega \approx S$ , so making it be in the order of units. In the example, we get  $\beta < \beta_0(2 \cdot 10^{-1} + 1 + 32/34) = 2.14\beta_0$ . In summary, the longer the TTC, the less relevant it becomes and we can keep the same gradient step even for long TTCs. On the contrary, with  $TTC_s$  in the example, we obtain  $\beta < 21.94\beta_0$ . That is,  $\sigma$  makes the TTC term be on the order of tens, with  $\omega \approx \frac{\sigma}{TTC_s}$ , which would even allow us to increase the gradient step to achieve quicker convergence.

- Second, the parameters establish the ratios of the allocated rates in presence of channel congestion as:

$$\frac{r_i}{r_j} \approx \left( \frac{w_i}{w_j} \right)^{\frac{1}{\alpha}} = \left( \frac{\frac{\sigma}{TTC_i} + 1 + \frac{v_i}{v_{MAX}}}{\frac{\sigma}{TTC_j} + 1 + \frac{v_j}{v_{MAX}}} \right)^{\frac{1}{\alpha}} \quad (10)$$

where  $TTC_x$  refers to the minimum TTC computed by vehicle  $x$ . For long TTCs, that is, in absence of substantial risk, the ratio is determined by the  $S$  term basically: For  $\alpha = 1$  and realistic speeds, the maximum ratio is around 2. Let us note how that ratio tends to 1 as  $\alpha$  increases, that is, as we argued previously, it tends to max-min fairness or more equal allocations. On the other hand, for short TTCs,  $\sigma$  again makes the maximum ratio depend basically on the ratio of the TTCs. Similarly, in the case of a short TTC and a long one, the former prevails over the  $S$  term.

In summary, with these parameters, we have an additional degree of control over the convergence speed and the allocations. In any case, we treat them as global parameters, in the sense that they do not need fine tuning. In our tests, we have set them to  $\sigma = 15$  and  $v_{MAX} = 34$  m/s, values which should work well in a very broad range of situations, legal limits and types of roads.

Thus, the updated procedure with respect to our previous algorithm in [6] is outlined in Algorithm 2.

---

**Algorithm 2** TTCC

---

```

1 Set initial vehicle prices  $\pi_v^0$  and rates  $r_v^0$ .
2 foreach interval  $k$  do
3   Each vehicle  $v$  receives  $\vec{A}_v^k, \vec{V}_v^k, \vec{P}_v^k, \pi_v^k, r_v^k$  from its
   neighbors  $n(v)$ .
4   At the end of interval  $k$ :
5   Compute the TTCs and store them in  $tcs$ :
6   for  $i$  in  $n(v)$  do
7      $TTC_{vi} \leftarrow$  Roots of eq. (6) for  $v$  and  $i$ ;
8      $tcs \leftarrow TTC_{vi}$ 
9   end
10  Get the minimum real positive root among  $tcs$ :
    $TTC_{min} \leftarrow \min(tcs \in \mathbb{R}^+)$ 
11  if  $\exists TTC_{min}$  then
12     $\omega_v \leftarrow \frac{\sigma}{TTC_{min}} + S$ 
13  else
14     $\omega_v \leftarrow S$ 
15  end
16  Then, each vehicle updates its rate  $r_v^k(\pi)$  according
   to:
17   $r_v^{k+1}(\pi) = \left[ \left( \frac{\omega_v}{\sum_{v' \in n(v)} \pi_{v'}^k} \right)^{\frac{1}{\alpha}} \right]_{R_v^{min}}^{R_v^{max}}$ 
18  Finally, each vehicle computes its new price:
19   $\pi_v^{k+1} = \left[ \pi_v^k - \beta \left( C - \sum_{v' \in n(v)} r_{v'}^k \right) \right]_0$ 
20 end

```

---

As shown in Algorithm 2, at regular  $k$  intervals, each vehicle collects both its current acceleration, speed, and position, and those of the neighboring vehicles from their corresponding received beacons. With this information, the vehicle under study computes the root of eq. (6) for each neighbor, which corresponds to the TTC for that neighbor.

If a collision is possible, at least one of these roots ( $t$ ) is real and positive. The TTC used in the algorithm is the minimum real positive root among all the obtained roots for all neighboring vehicles. The remaining steps of the iteration are identical to those of [6] and solve the problem (1) in a distributed way. We finish this section with a clarification of some features of TTCC:

- The procedure is *local and fully distributed*. Each vehicle independently sets its priority  $\omega_v$  with the information received from one-hop neighbors. Similarly, the

weights and rates are computed with only local information from one-hop vehicles.

- The information required for TTCs: position, velocity, and acceleration can be extracted from the fields already present in the beacons; specified in the standards. The only additional information each vehicle has to insert in a beacon, required to solve the NUM problem, is the weight ( $\pi$ ) and, optionally,<sup>2</sup> rate ( $r$ ); just two real numbers. This small overhead is similar to other proposals, such as LIMERIC+PULSAR, which requires the sending of two real numbers, local and one-hop Channel Busy Ratio (CBR).
- Let us remark that priorities are only enforced if there is not enough capacity, as shown in Fig. 1c. If the MBL constraint is not active, that is, the load is below MBL, the beaconing rates are always set to the maximum rate,  $R_{max}$ , for all vehicles.

### V. RESULTS

In this section, we evaluate the performance of the TTCC versus other approaches previously discussed, namely: (i) LIMERIC+PULSAR, as a pure CC solution, (ii) CAM-DCC, specified in the standards with AC and CC, (iii) EMBARC, which integrates AC with LIMERIC, and (iv) NORAC, an integrated AC and CC solution based on game theory which provides weighted fairness. Unless explicitly mentioned, all the simulations have been made with OMNeT++ 5.3 [36] and its INET 3.5 library [40], which implements the IEEE 802.11p standard and realistic propagation and interference models, also considering the capture effect. An additional mobility module, which implements the Intelligent Driver Model (IDM), has been developed to simulate more realistic driver behavior [41].

In Table 1, we summarize the simulation parameters, common to the simulation studies in this and the following section. We use a 6 Mbps channel and a beacon size of 500 bytes, which gives a total message size of 536 bytes including the MAC headers, and according to [20], the resulting PHY packet duration is 760  $\mu$ s. With these channel settings, the MBL constraint is set to  $C = 789.47$  beacons/s to reserve 40% of the capacity for the DEN service, as explained in previous sections. In the particular case of NORAC, the utility parameter has been set, as a reference, to  $u_v = \lfloor v_v/4 \rfloor_4$ , being  $u_v$  the speed of each vehicle  $v$ . As we discussed in Sect. II, an intrinsic problem of NORAC is that it requires adjusting a proper combination of parameters for different scenarios. Following the scheme of the authors in [10], we have tested  $\lfloor u_v \rfloor_4$  and  $\lfloor u_v/2 \rfloor_4$ , but since the maximum speed for which they tested the algorithm is 20 m/s, the

TABLE 1. OMNet++ simulation parameters.

Algorithm	Parameter	Value
*	Frequency (f)	5.9 GHz
*	Power (P)	251 mW
*	Sensitivity (S)	-92 dBm
*	Data rate (D)	6 Mb/s
*	SNIR Threshold (T)	4 dB
*	Background Noise (N)	-110 dBm
*	Path loss	Nakagami-m
*	Old neighbor removal	5 s
*	Beacon duration	760 $\mu$ s
*	Capacity (C)	789.47 beacons/s
*	Maximum rate ( $R_v^{max}$ )	10 Hz
*	Minimum rate ( $R_v^{min}$ )	1 Hz
TTCC	$\pi_v^0$	$1.252 \times 10^{-3}$
TTCC	$r_v^0$	5 Hz
TTCC	$\alpha$	1
TTCC	$\beta_F$	$2.8 \times 10^{-7}$
LIMERIC (+PULSAR)	$\alpha_L$	0.1
LIMERIC (+PULSAR)	$\beta_L$	1/150
LIMERIC+PULSAR	CMDI	300 ms
CAM-DCC	$T\_CheckGenCam$	10 ms
CAM-DCC	$N\_GenCam$	3
EMBARC	$\alpha_L$	0.1
EMBARC	$\beta_L$	1/400
EMBARC	$T'$	0.2 m
EMBARC	$\delta_s$	100 ms
EMBARC	$\delta_t$	300 ms
NORAC	$u_v$	$\lfloor v_v/4 \rfloor_4$
NORAC	$p_{c_v}$	0.6, 1.0

\* Common parameters for all the algorithms.

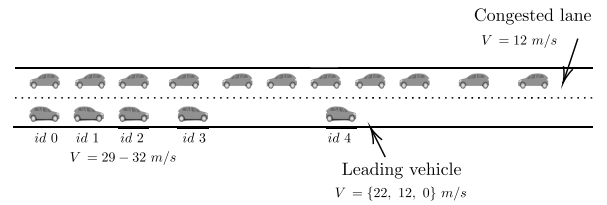


FIGURE 5. Free-flow direction scenario with all vehicles in range and leading vehicle 4 limiting the speed.

resulting beaconing rates are too high when we now employ higher speeds (e.g. 20-34 m/s) and the MBL constraint is not met. Other functions could be introduced, such as our own TTC, but further parameter adjustment would be required.

### A. CONGESTED AND FREE-FLOW DIRECTIONS WITH ALL VEHICLES IN RANGE

In the first scenario, we set up 5 consecutive vehicles in movement on a lane at high speeds, and other parallel lanes in the opposite direction with a traffic jam to induce channel congestion. We call this the congested/free-flow direction scenario. The first group is led by the vehicle with ID = 4 (vehicle 4, hereinafter), which has a lower speed than vehicles 0, 1, 2 and 3, as shown in Table 2 and Fig. 5. With the implemented IDM model, such initial differences in speed and separation force the following vehicles to decelerate with different intensity.

We intend to show the effect of vehicle deceleration on the beaconing rate. This is a situation where the TTC of

<sup>2</sup>The algorithm requires that each vehicle know the load it measures in the channel, which is either the sum of the rates or approximately equal to the CBR. Therefore, only the weights need to be broadcast and CBR can be locally measured. We prefer to send the rate because it generally tends to be more stable. When the CBR is not equal to the sum of the rates, for instance in cases of severe fading, using the measured CBR allows us to adjust the allocation better to the actual channel load. Otherwise, in those cases, the load is overestimated and the allocation is slightly below the optimal.

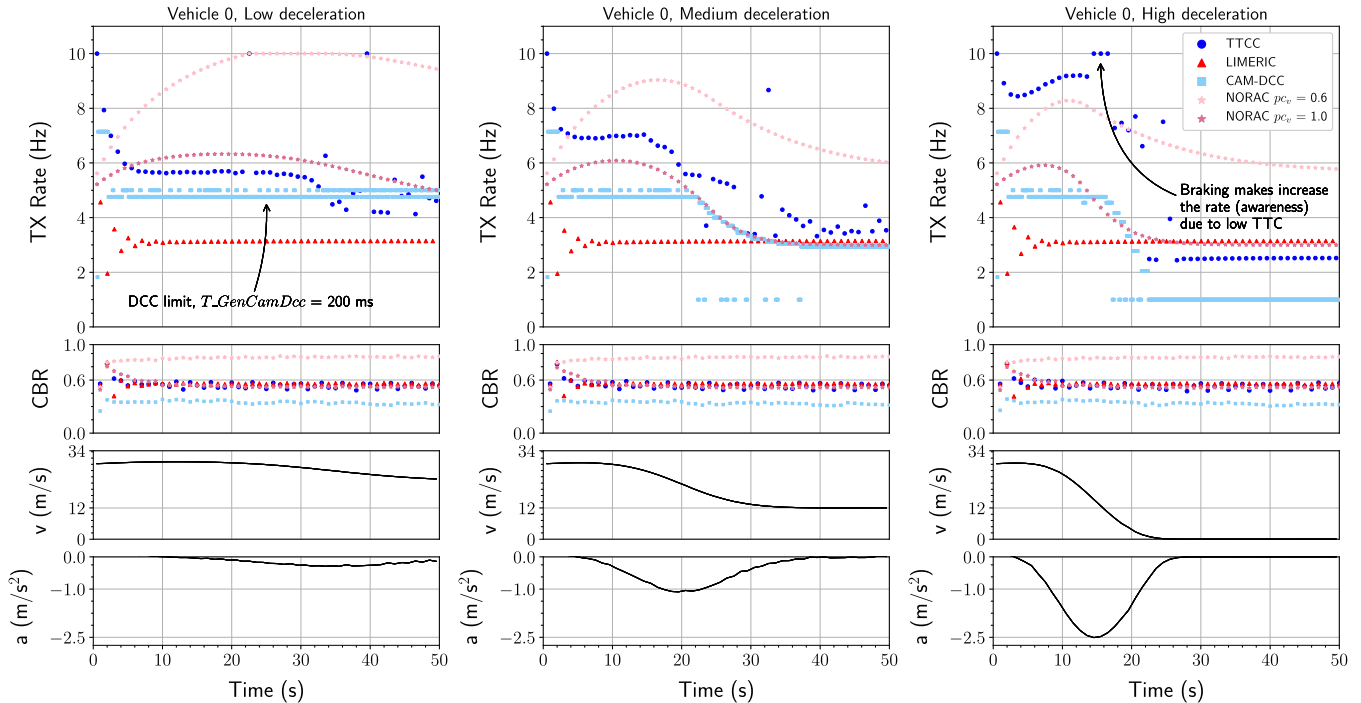


**FIGURE 6.** Rate control approaches comparative for vehicle 0, evaluated in different deceleration cases being all vehicles in range. From top to bottom: beaconing rate, channel busy rate, velocity and deceleration.

**TABLE 2.** Simple scenario, initial positions and speeds.

Vehicle ID	0	1	2	3	4	5	...	235
$v_0$ (m/s)	29	30	31	32	22, 12, 0*	12	...	12
$x_0$ (m)	15	60	130	210	450	5	...	1996
$y_0$ (m)	8	8	8	8	8	15	...	15

\* Variable employed to generate different deceleration cases.

the following vehicles must increase due to a risky situation created by the slower leading vehicle. Note that the vehicles in the traffic jam are not stopped, but moving at a slow uniform speed of 12 m/s, to prevent CAM-DCC from decreasing the beaconing rate down to one. They have been randomly positioned according to a Poisson distribution of average density  $\rho = 0.14$  vehicles/m. There is a total of 236 vehicles in the network, all in range of each other. A Nakagami-m propagation model is used, and, as a consequence, the packet reception is not deterministic. The average carrier sense range [42] for this scenario is 1805 m, corresponding to a shape parameter  $m = 2$  and path loss exponent  $\beta_{PL} = 2$ .

In Figure 6, we show the results for vehicle 0, the last of the high-speed vehicles, for 50 seconds and three different deceleration profiles, corresponding to IDM behavior in response to the initial speed of the leading vehicle 4. In the first case, where this speed is set at 22 m/s, we obtain light deceleration, which corresponds to a natural driver fit of the optimal speed in the road and which barely entails risk. Secondly, the initial speed of the leading vehicle is set at 12 m/s, which results in a moderate deceleration and risk; and finally, abrupt deceleration of about  $-3 \text{ m/s}^2$  is forced when the leading vehicle is completely stopped.

As might be expected, LIMERIC does not take the movement of the vehicle into account and allocates resources only according to the locally measured CBR. Particularly, with 236 vehicles all in range, all rates go to 3.668 Hz, which is an equal share of the available bandwidth.

Regarding CAM-DCC, it triggers a new CAM generation when there have been certain variations in speed, heading, or position during the last interval. That is, it reacts to the dynamics of the vehicle. It is always limited by the DCC entity, which constrains the CAM rate according to the congestion measured in the channel by a finite state machine, as in [4], [8], [21]. Results show that for the CAM-DCC algorithm, the speed of the vehicle proportionally determines the beaconing rate until it is limited by the DCC entity. In Fig. 6, we can see that even though the velocity is still high, the beaconing rate drops to 5 beacons/s ( $T\_GenCamDcc = 200 \text{ ms}$ ) due to the CBR limit, as a result of the CBR created by the vehicles in the congested direction, not shown in the aforementioned figure, but which have a similar rate to those of LIMERIC. This is an unnecessary limitation for a vehicle in a potentially unsafe situation; even more so when the CBR is only slightly above 0.3 and there is ample margin before reaching the MBL. In the moderate and sudden deceleration cases, again the DCC entity unnecessarily prevents the vehicle from raising the rate above 5 beacons/s. Moreover, the rate decreases as the speed decreases, independently of the traffic situation. The appropriateness of this behavior is questionable, as a vehicle stopped in the middle of a highway would transmit at just 1 beacon/s, oblivious to the state of the rest of vehicles, and in fact, this case is questioned in the standards

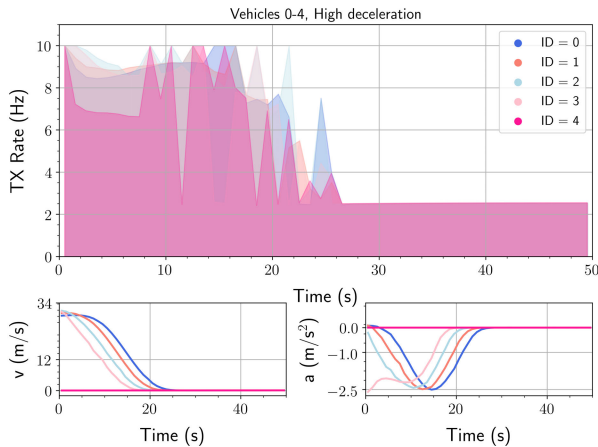


**FIGURE 7.** TTCC rate control for vehicles 0-4 evaluated in the high-decelerated case, with all vehicles in range with each other and leading vehicle 4 limiting the speed.

for safety applications [17, Annex F]. On the contrary, TTCC effectively takes into account the surrounding traffic situation and prevents this issue: with TTCC, vehicle 4, the leading one, also keeps a higher rate. Especially, in the case of high deceleration, where it is completely stopped, it still keeps a high rate until the risk is over, as shown in Fig. 7.

The behavior of NORAC depends on the combination of parameters, as we commented. The beaconing rate results are in accordance with CAM-DCC, except that setting the lower limit of speed to 4 m/s avoids dropping the rate to 1 Hz. But depending on the value of the price, the MBL may be violated, for instance, when using the recommended values in [10], or when establishing  $pc_v = 0.6$ . As shown in the next sections, NORAC requires its parameters to be tuned for each road scenario.

With TTCC, however, the beaconing rate adjusts to the risk of the situation, while keeping the CBR at the desired limit. In all the cases, as an example of weighted fairness in action, the  $\omega$  parameter makes the beaconing rate of the free-flow vehicles stay well above the vehicles in the direction of the traffic jam, which are transmitting at around 3.5 beacon/s. That is, they have reduced their rates slightly to allow for the increase of the beaconing rates of the vehicles in the high-speed direction. Moreover, in the case of abrupt deceleration, it may seem odd that vehicle 0 sets the rate below 3.66 beacon/s, but, in fact, this is intended behavior. Since after  $t = 25$  s, all the vehicles in the high-speed direction are stopped, there is actually no risk; that is, no TTC and  $\omega = 1$ , whereas the vehicles in the jammed direction are moving at 12 m/s, so their  $\omega > 1$  and they transmit at around 3.5 beacon/s.

As a final remark, the CBR for TTCC is always slightly below the 0.6 limit because of the algorithm implementation. At step 15 of Algorithm 1, to compute the difference between the MBL and the load, vehicles use the beaconing rate that their neighbors are using piggybacked in the received beacons. But, due to the fading of the propagation model, some of those beacons are lost. LIMERIC, however, adjusts to the

MBL better because it uses the measured CBR. If a more precise fitting were necessary, TTCC could also compare the MBL to the measured CBR in step 15.

**B. CONGESTED AND FREE-FLOW DIRECTIONS WITH MULTI-HOP**

This scenario is the same as the previous one, but in this case, we change the path loss exponent of the Nakagami-m propagation from 2 to 2.5, which reduces the transmission range from 1805 to 403 m, approximately. Unlike the previous case, the vehicles have a different number of neighbors in range depending on their position, and so they set different beaconing rates depending on their position. We evaluate the sudden deceleration scenario.

In Figure 8a, we plot the time evolution of the beaconing rate, CBR, and the number of neighbors, while in Fig. 8b, we plot the beaconing rate and CBR vs the position of all the vehicles at  $t = 15$  s, because from Fig. 6, the greatest deceleration occurs approximately at that time. Regarding the overall rate allocation, in Fig. 8b, we can see how CAM-DCC only assigns a rate of 3 beacons/s proportional to vehicle speeds, which results in an under-use of the capacity, with CBR below 0.2. Unlike the all-in-range scenario, the DCC limit is not met in this case, and so we can observe in Fig. 8a, that the decelerating vehicle can set a higher beaconing rate in the interval from 0 to 18 s. LIMERIC+PULSAR (shown as L+P), NORAC and TTCC try to maximize the capacity up to the MBL. In the case of TTCC, we can see the typical “U” allocation for proportional fairness [6], where the throughput is being maximized when possible. So the vehicles on the edges of the scenario set a much higher rate, since they have fewer neighbors and therefore, experience less load. LIMERIC+PULSAR, on the contrary, yields a typical max-min allocation, and so the bottleneck links, in this case, the vehicles in the middle of the scenario, limit the maximum rate for the others: all vehicles set their rate equal to the rate of the more loaded ones. This is the typical trade-off between resource usage and fairness, which manifests itself also as a CBR below the MBL.

If we look at the time evolution for vehicle 0, we see that the LIMERIC+PULSAR beaconing rate goes to the common final allocation with a slight oscillation, independently of the dynamics of the vehicle. TTCC, on the contrary, keeps the beaconing rate to a maximum due to the risk, and only when it is over is it decreased to the level of the neighbors in the congested area. Later, as the congested cluster moves away, the beaconing rate is raised again, contrary to LIMERIC+PULSAR, which maintains the rate of the most congested vehicle level as long as there is a multi-hop link to the bottlenecked area. Concerning NORAC, we use the same utility and price parameters than in the previous scenario, where using  $pc_v = 0.6$  resulted in a remarkable surpassing of the MBL. But, nevertheless, in this case, makes the CBR keep below the MBL. This outcome confirms again that NORAC requires fine parameter tuning for different scenarios or a more clear selection procedure.

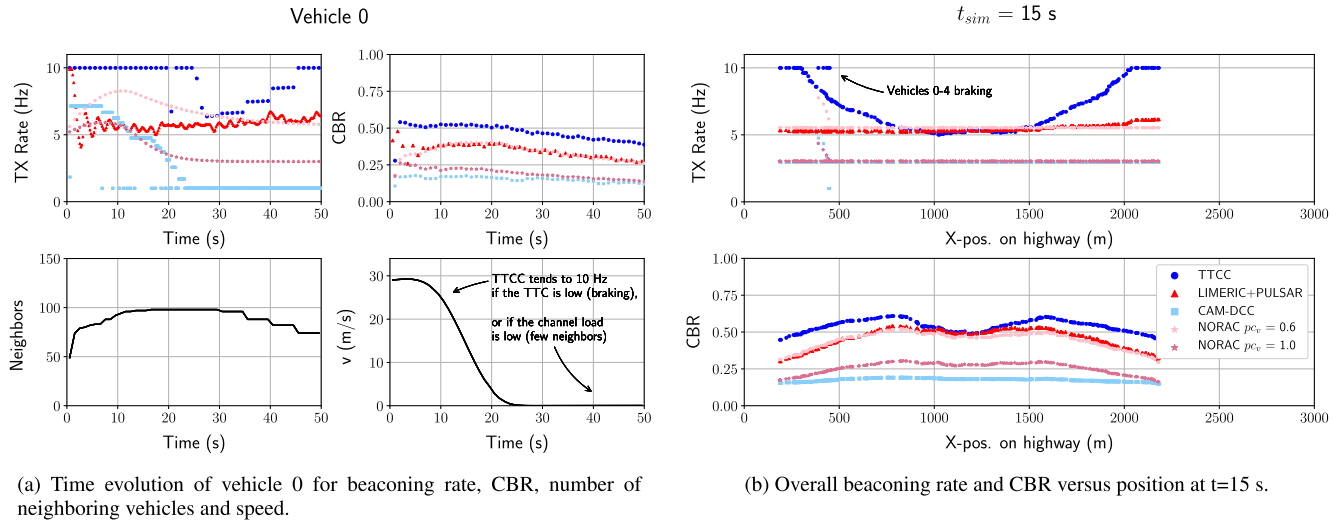


FIGURE 8. Congested/free-flow direction scenario with multiple hops.

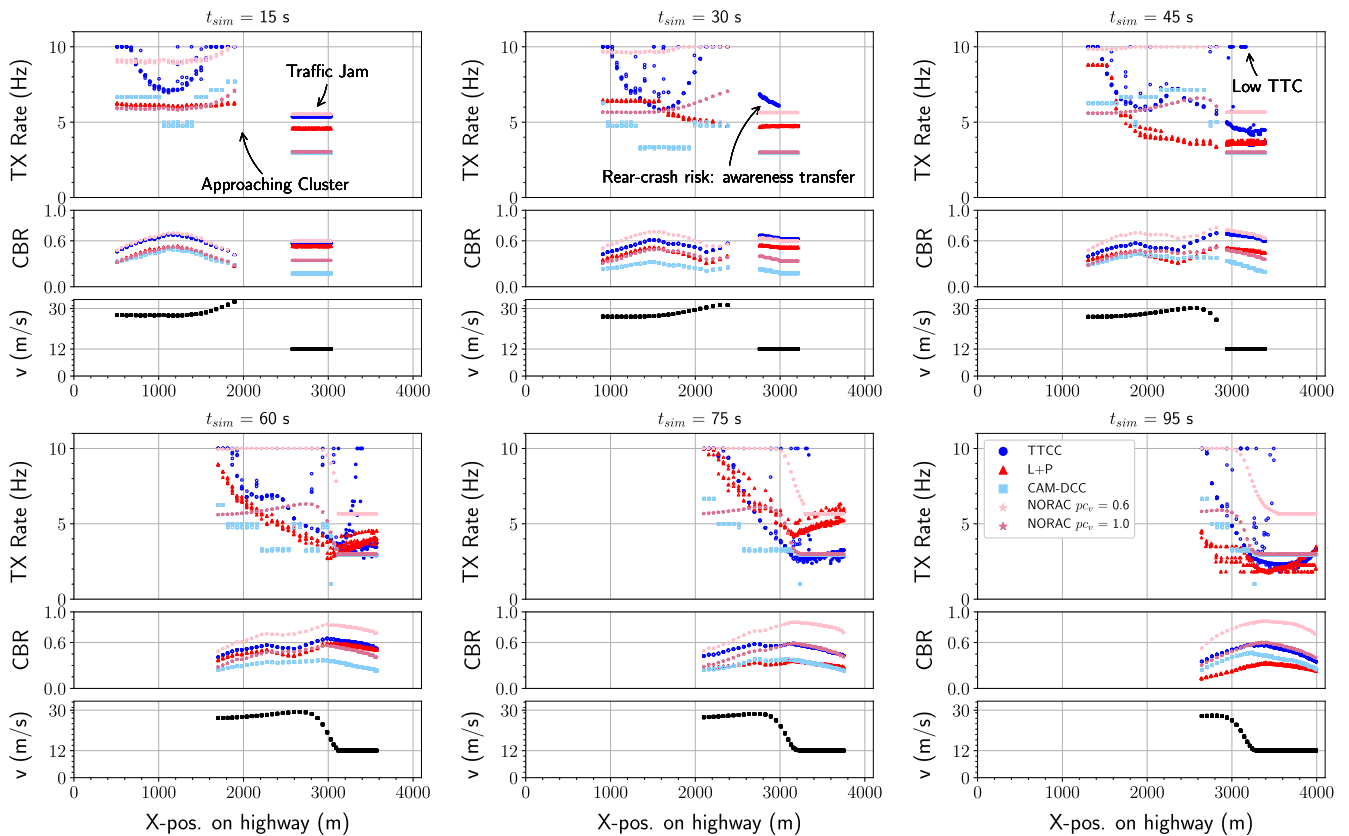


FIGURE 9. Comparison of different beaoning rate control algorithms in a realistic scenario with a cluster of moving vehicles approaching a traffic jam.

We have also simulated EMBARC in this scenario. However, the results are very similar to those of LIMERIC+PULSAR, because the tracking error does not change noticeably in this scenario, and so no additional beacon is triggered. Once the main features of both congestion and awareness control both for all the vehicles in range and multi-hop for a simple scenario have been analyzed, we turn to

evaluate a more realistic road situation, consisting of a large number of vehicles in motion.

### C. REALISTIC TRAFFIC JAM WITH MULTI-HOP

To observe the TTCC response in a real scenario with a large number of moving vehicles, we generate two approaching clusters of vehicles: one (Cluster A) at very high speed

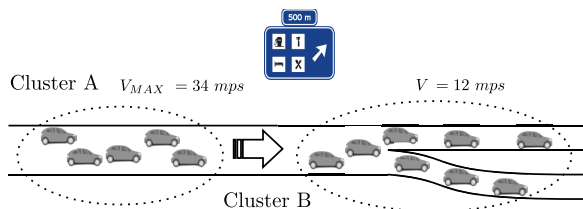


**FIGURE 10.** Realistic multi-hop scenario consisting of moving cluster approaching a jammed area.

**TABLE 3.** Realistic traffic jam scenario, initial positions, and speeds.

Vehicle ID	0, 1, 2	...	147, 148, 149	150, 151, 152	...	297, 298, 299
$v_0$ (m/s)	34	...	34	12	...	12
$x_0$ (m)	20	...	1285	2294	...	2641
$y_0$ (m)	5, 8, 11	...	5, 8, 11	5, 8, 11	...	5, 8, 11

( $V_{MAX} = 34$  m/s) and another (Cluster B) congested due to a traffic jam (12 m/s), as depicted in Figure 10. We now require more realistic separation distances. Otherwise, the TTC would yield values that are too low. Therefore, we position the vehicles according to a Poisson process, separating vehicles with distances of between 10 and 40 m for those in free flow and distances of between 5 and 10 m for those located in the congested road section. In addition, we introduce channel congestion by adding 2 more lanes in different y-axis positions. Altogether, we have 300 vehicles, divided into two clusters of 150 vehicles each, separated by 1000 m, as shown in Table 3. This distance is introduced for two reasons: (i) to give the algorithms time to converge and leave the transient phase, and (ii) to clearly observe the priority of speed before the vehicles start to measure risk and, therefore, the TTC priority mechanism is applied. The transmission range used in this section is set at 403 m as in the previous scenario. In Figure 9, the beaconing rate is plotted versus the position of the vehicles for different simulation times to allow us to observe the channel management and behavior of each studied approach. In addition, we show the speed versus position of the vehicles to discuss their influence.

*15 seconds*

In the first 15 seconds, when the clusters are still isolated, we see a typical allocation pattern in a multi-hop scenario for TTCC for the approaching cluster, with higher speed vehicles prioritized. In contrast, the allocation is flatter for the other proposals, equal for LIMERIC+PULSAR, and proportional to speed for NORAC and CAM-DCC, except in this latter for the middle of the approaching cluster, where a higher load triggers the DCC entity, which limits the rates to 5 beacon/s. In the congested flow cluster, since all the vehicles are in range due to higher vehicle density, all the proposals result in a flat rate allocation, but TTCC and NORAC set a higher value due to its design.

*30, 45 seconds*

As time passes, some leading vehicles from the front of the moving cluster start entering the range of those located

in the traffic jam. For TTCC, the approaching vehicles start detecting the jam and the risk involved, so the TTCs begin to decrease, while the rates increase. The effect is more clearly visible in the front section of the congested cluster, marked with an arrow in the figure, where the risk assessed as TTC makes the vehicles increase their rates, balanced by a decrease in the rates of vehicles in the rear section. This is a behavior not shared by other proposals and shows how weighted fairness operates in TTCC.

In this interval, the speed is still high because free-flow vehicles are far from the congested cluster. However, they are already in communication range, and the measured channel load increases, which triggers the DCC limit for CAM-DCC and forces vehicles to decrease their rates. This behavior is questionable, since high speed, potentially more risky vehicles are forced to reduce their rates unnecessarily. NORAC solves this point by keeping high the beaconing rates until vehicles begin braking. With LIMERIC+PULSAR, the rates are directly reduced to match those of the congested cluster. Again, the max-min approach forces vehicles to adopt the rate of the most congested link.

*60, 75, 95 seconds*

When the approaching cluster of vehicles comes close to the traffic jam, the risk of collision is more significant due to a low relative distance and a high relative speed. TTCC increases the rates of the vehicles involved to a maximum, shown in Figure 9 between 2600 and 3400 m. Over time, as drivers brake, the risk of collision is gradually moving along the cluster, from the front (3500-4000 m) to rear (1800-2600 m), depending on the measured TTC at each moment. Also, as more vehicles join the congested queue, the channel load increases. TTCC forces beaconing rates to decrease gradually along the merging clusters, lowering the rates of those in the queue without risk and keeping the rates of both vehicles with low risk high or not really measuring congestion on the channel. In comparison, LIMERIC+PULSAR cause the rates to drop more drastically and with oscillations, shown in  $t = 60, 75,$  and  $90$  s. CAM-DCC again tracks the speed in the sense that it assigns rates proportionally to speed in general, decreasing the rate as the vehicles brake. Similarly, NORAC decreases the beaconing rate in function of the vehicle speed, but, as the number of neighboring vehicles increases, the CBR may grow also without any limitation or not, again depending on the selected value of the price parameter.

**D. GRID ROAD**

Finally, we test TTCC in a scenario with intersections, where vehicles approach intersections at different speeds and stop in queues before crossing them, according to their right of way. We have used SUMO [43] to simulate realistic traffic patterns. We have set up a  $2 \times 2$  grid road network with 9 intersections and 600 m edges with 4 lanes each, where vehicles tend to a top speed of 34 m/s whenever possible and no other vehicle is ahead. The minimum distance traveled for each vehicle has been set at 12 km with 15 intermediate

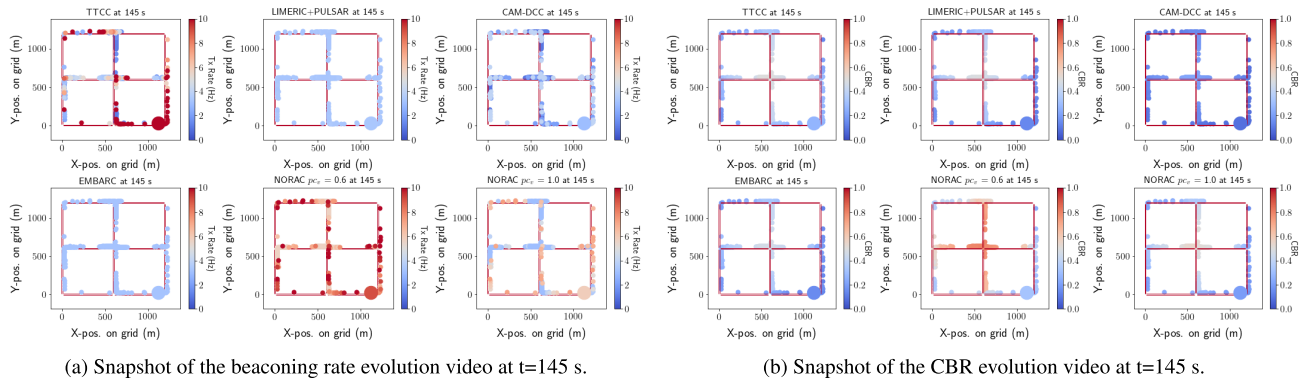


FIGURE 11. Grid scenario with multihop range. Vehicle 192 highlighted with a larger marker.

TABLE 4. SUMO configuration.

Parameter	Value
Grid number	3
Grid length	600 m
Default speed	34 m/s
Lanes	4
Trip beginning time	0 s
Trip ending time	10 s
Repetition rate	0.03 s
Minimum distance	12 km
Intermediate way-points	15
Fringe factor	100

way-points, which allows us to record the same number of data once the algorithm is stable (from 150 s to 450 s). The number of vehicles is fixed in the network since all of them have already been inserted and neither has completed their trip. A summary of the SUMO simulation parameters is shown in Table 4. We have tested TTCC, LIMERIC+PULSAR, CAM-DCC, NORAC, and EMBARC.

Due to the multidimensional nature of the results of this scenario and the difficulties of drawing them on a picture, we have included supplementary videos (MPEG4 files) which show the time evolution for the beaoning rate and CBR on the road overlay. A sample image is shown in Fig. 11, and the videos will be available at <http://ieeexplore.ieee.org>. As can be seen, TTCC vehicles typically set their maximum beaoning rate on clear road sections, as well as when they approach intersections. While vehicles are stopped on queues, they tend to reduce their beaoning rate unless they detect a potentially dangerous approaching vehicle. LIMERIC+PULSAR, being a pure CC algorithm, keeps an almost constant beaoning rate independently of the road section and traffic situation, whereas CAM-DCC and NORAC basically set the beaoning rate proportional to the speed. Although not shown either in the video or in Figure 12, if we combine CAM-DCC with LIMERIC+PULSAR, the results are very similar, because the beacon generation is separate from the CC and the latter only limits the maximum rate. The results for EMBARC are very similar to those of LIMERIC+PULSAR and only some additional beacons are

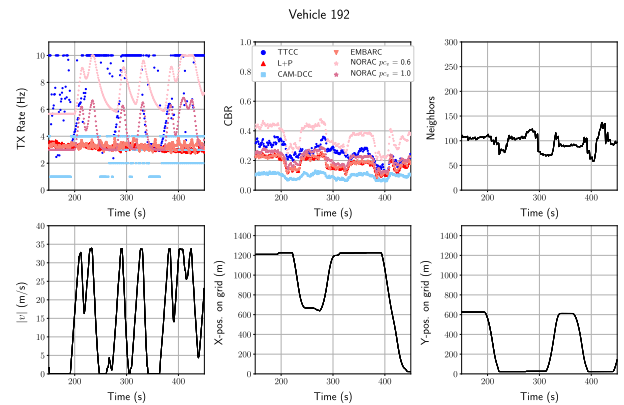


FIGURE 12. Comparison of different beaoning rate control algorithms with SUMO in a grid scenario for a representative vehicle (192).

sent when the suspected tracking error of the vehicles reach a certain threshold ( $T' = 0.2$  m), which occurs when vehicles are turning, braking, or accelerating. Nevertheless, this mentioned extra transmission does not occur very often (see Fig. 12) with a representative vehicle with id = 192, which confirms that it is only active in noticeable curvy scenarios.

Overall, as shown in Fig. 12, TTCC vehicles maintain a higher beaoning rate, often the maximum, for longer times, without violating the MBL, which should always benefit the QoS of applications on top of the service. In the case of NORAC, given the number of vehicles implied and the given speeds, this is also satisfied, since the CBR is above average but the MBL is not exceeded. EMBARC, on the other hand, oscillates unless we set its  $\beta_L$  parameter to 1/400 [5], which stabilizes the control, but results in an unnecessarily low beaoning rate, even though the CBR is not close to the MBL.

## VI. CONCLUSION

We have described and discussed TTCC, integrated awareness and congestion control algorithm based on distributed Network Utility Maximization (NUM). TTCC keeps the channel load under a given threshold while assessing the safety of the surrounding traffic situation with a time-to-collision metric, valid in general traffic situations, which is

used to assign priorities in the optimal allocation problem. This simple, but general vector formulation for TTC is one of the distinctive features of TTCC. It allows us to seamlessly assess the risk in curves and intersections and aligns well with the CAM management alternatives discussed in European safety signaling standards.

Results show that TTCC effectively raises the beaconing rate of the vehicles involved in more dangerous situations, and, in general, TTCC yields higher rates and better usage of channel capacity. In any case, its behavior can be further tuned through the  $\sigma$  parameter to be more or less sensitive to the computed TTC. As for the next steps, we intend to continue evaluating the suitability of the metric and parameters regarding the risk of the surrounding traffic situation. Finally, we plan to study how to integrate our control in multi-access scenarios with cellular communications.

## ACKNOWLEDGMENT

The authors would like to thank Adegoke Oluwaseyi and Bharath Raj for their support and advice on the rendered 3D video and animation.

## REFERENCES

- [1] J. Guanetti, Y. Kim, and F. Borrelli, "Control of connected and automated vehicles: State of the art and future challenges," *Annu. Rev. Control*, vol. 45, pp. 18–40, May 2018.
- [2] K. C. Dey, L. Yan, X. Wang, Y. Wang, H. Shen, M. Chowdhury, L. Yu, C. Qiu, and V. Soundararaj, "A review of communication, driver characteristics, and controls aspects of cooperative adaptive cruise control (CACC)," *IEEE Trans. Intell. Transp. Syst.*, vol. 17, no. 2, pp. 491–509, Feb. 2016.
- [3] A. Vahidi and A. Eskandarian, "Research advances in intelligent collision avoidance and adaptive cruise control," *IEEE Trans. Intell. Transp. Syst.*, vol. 4, no. 3, pp. 143–153, Sep. 2003.
- [4] *Intelligent Transport Systems (Its); Vehicular Communications; Basic Set of Applications; Part 2: Specification of Cooperative Awareness Basic Service*, Standard ETSI-EN 302 637-2 v1.4.1, ETSI, Aug./Sep. 2019.
- [5] G. Bansal, J. B. Kenney, and C. E. Rohrs, "LIMERIC: A linear adaptive message rate algorithm for DSRC congestion control," *IEEE Trans. Veh. Technol.*, vol. 62, no. 9, pp. 4182–4197, Nov. 2013.
- [6] E. Egea-Lopez and P. P. Mariño, "Distributed and fair beaconing rate adaptation for congestion control in vehicular networks," *IEEE Trans. Mobile Comput.*, vol. 15, no. 12, pp. 3028–3041, Dec. 2016.
- [7] Y. P. Fallah, C.-L. Huang, R. Sengupta, and H. Krishnan, "Analysis of information dissemination in vehicular ad-hoc networks with application to cooperative vehicle safety systems," *IEEE Trans. Veh. Technol.*, vol. 60, no. 1, pp. 233–247, Jan. 2011.
- [8] A. Rostami, B. Cheng, G. Bansal, and K. Sjöberg, M. Gruteser, and J. B. Kenney, "Stability challenges and enhancements for vehicular channel congestion control approaches," *IEEE Trans. Intell. Transp. Syst.*, vol. 17, no. 10, pp. 2935–2948, Oct. 2016.
- [9] N. Lyamin, A. Vinel, M. Jonsson, and B. Bellalta, "Cooperative awareness in VANETs: On ETSI EN 302 637-2 performance," *IEEE Trans. Veh. Technol.*, vol. 67, no. 1, pp. 17–28, Jan. 2018.
- [10] F. Goudarzi and H. Asgari, "Non-cooperative beacon rate and awareness control for vanets," *IEEE Access*, vol. 5, pp. 16858–16870, 2017.
- [11] M. Sepulcre, J. Mittag, P. Santi, H. Hartenstein, and J. Gozalvez, "Congestion and awareness control in cooperative vehicular systems," *Proc. IEEE*, vol. 99, no. 7, pp. 1260–1279, Jul. 2011.
- [12] M. Sepulcre, J. Gozalvez, O. Altintas, and H. Krems, "Integration of congestion and awareness control in vehicular networks," *Ad Hoc Netw.*, vol. 37, pp. 29–43, Feb. 2016.
- [13] S. Joerer, B. Bloessl, M. Segata, C. Sommer, R. L. Cigno, A. Jamalipour, and F. Dressler, "Enabling situation awareness at intersections for IVC congestion control mechanisms," *IEEE Trans. Mobile Comput.*, vol. 15, no. 7, pp. 1674–1685, Jul. 2016.
- [14] G. Bansal, H. Lu, J. B. Kenney, and C. Poellabauer, "Embarc: Error model based adaptive rate control for vehicle-to-vehicle communications," in *Proc. 10th ACM Int. Workshop Veh. Inter-Netw., Syst., Appl.*, Jun. 2013, pp. 41–50.
- [15] F. Goudarzi, H. Asgari, and H. S. Al-Raweshidy, "Fair and stable joint beacon frequency and power control for connected vehicles," in *Proc. Wireless Netw.*, 2019, pp. 1–12.
- [16] *Intelligent Transport Systems (Its); Cross Layer DCC Management Entity for Operation in the Its G5A and Its G5B Medium*, Standard ETSI Ts 103 175 v1.1.1, ETSI, Jun. 2015.
- [17] *Intelligent Transport Systems (Its); V2x Applications; Part 1: Road Hazard Signalling (RHS) Application Requirements Specification*, Standard ETSI Ts 101 539-1 v1.1.1, ETSI, Aug. 2013.
- [18] *Intelligent Transport Systems (Its); V2x Applications; Part 2: Intersection Collision Risk Warning (ICRW) Application Requirements Specification*, Standard ETSI Ts 101 539-2 v1.1.1, ETSI, Jun. 2018.
- [19] *Intelligent Transport Systems (Its); V2x Applications; Part 3: Longitudinal Collision Risk Warning (LCRW) Application Requirements Specification*, Standard ETSI Ts 101 539-3 v1.1.1, ETSI, Nov. 2013.
- [20] *Intelligent Transport Systems (Its); Access Layer Specification For Intelligent Transport Systems Operating in the 5 GHz Frequency Band*, Standard ETSI En 302 663 v1.3.0, ETSI, May 2019.
- [21] *Intelligent Transport Systems (Its); Cross Layer DCC Management Entity For Operation in the Its G5A and its G5B Medium; Validation Set-Up and Results*, Standard ETSI Tr 101 613 v1.1.1, ETSI, 2015.
- [22] T. Lorenzen and H. Tchouankem, "Evaluation of an awareness control algorithm for VANETs based on ETSI EN 302 637-2 V1.3.2," in *Proc. IEEE Int. Conf. Commun. Workshop (ICCW)*, Jun. 2015, pp. 2458–2464.
- [23] E. Egea-Lopez, "Fair distributed congestion control with transmit power for vehicular networks," in *Proc. IEEE 17th Int. Symp. World Wireless, Mobile Multimedia Netw. (WoWMoM)*, Jun. 2016, pp. 1–6.
- [24] E. Egea-Lopez and P. Pavon-Mariño, "Fair congestion control in vehicular networks with beaconing rate adaptation at multiple transmit powers," *IEEE Trans. Veh. Technol.*, vol. 65, no. 6, pp. 3888–3903, Jun. 2016.
- [25] T. Tielert, D. Jiang, Q. Chen, L. Delgrossi, and H. Hartenstein, "Design methodology and evaluation of rate adaptation based congestion control for vehicle safety communications," in *Proc. IEEE Veh. Netw. Conf. (VNC)*, Nov. 2011, pp. 116–123.
- [26] J. Kenney, D. Jiang, G. Bansal, and T. Tielert, "Controlling channel congestion using cam message generation rate," in *Proc. 5th ETSI ITS Workshop*, 2013.
- [27] H.-H. Nguyen and H.-Y. Jeong, "Mobility-adaptive beacon broadcast for vehicular cooperative safety-critical applications," *IEEE Trans. Intell. Transp. Syst.*, vol. 19, no. 6, pp. 1996–2010, Jun. 2018.
- [28] *J2945/1: On-Board System Requirements for V2V Safety Communications—SAE International*, SAE International, Warrendale, PA, USA, 2019.
- [29] F. Lyu, H. Zhu, N. Cheng, Y. Zhu, H. Zhou, W. Xu, G. Xue, and M. Li, "ABC: Adaptive beacon control for rear-end collision avoidance in VANETs," in *Proc. 15th Annu. IEEE Int. Conf. Sens., Commun., Netw. (SECON)*, Jun. 2018, pp. 1–9.
- [30] A. Dayal, E. Colbert, V. Marojevic, and J. Reed, "Risk controlled beacon transmission in v2v communications," in *Proc. IEEE 89th Veh. Technol. Conf. (VTC-Spring)*, Apr./May 2019, pp. 1–6.
- [31] F. Kelly, "Charging and rate control for elastic traffic," *Eur. Trans. Telecommun.*, vol. 8, no. 1, pp. 33–37, Jan./Feb. 1997.
- [32] J. Mo and J. Walrand, "Fair end-to-end window-based congestion control," *IEEE/ACM Trans. Netw.*, vol. 8, no. 5, pp. 556–567, Oct. 2000.
- [33] L. Zhang and S. Valaee, "Congestion control for vehicular networks with safety-awareness," *IEEE/ACM Trans. Netw.*, vol. 24, no. 6, pp. 3290–3299, Dec. 2016.
- [34] M. Sepulcre, J. Gozalvez, and B. Coll-Perales, "Why 6 Mbps is not (always) the optimum data rate for beaconing in vehicular networks," *IEEE Trans. Mobile Comput.*, vol. 16, no. 12, pp. 3568–3579, Apr. 2017.
- [35] S. Subramanian, M. Werner, S. Liu, J. Jose, R. Lupoiae, and X. Wu, "Congestion control for vehicular safety: Synchronous and asynchronous mac algorithms," in *Proc. 9th ACM Int. Workshop Veh. Inter-Netw., Syst., Appl.*, Jun. 2012, pp. 63–72.
- [36] A. Varga, "OMNeT++," in *Modeling Tools Network Simulation*. Berlin, Germany: Springer, 2010, pp. 35–59.
- [37] S. H. Low and D. E. Lapsley, "Optimization flow control. I. Basic algorithm and convergence," *IEEE/ACM Trans. Netw.*, vol. 7, no. 6, pp. 861–874, Dec. 1999.



- [38] M. Sepulcre and J. Gozalvez, "Coordination of congestion and awareness control in vehicular networks," *Electronics*, vol. 7, no. 11, p. 335, Nov. 2018.
- [39] S. E. Shladover and S.-K. Tan, "Analysis of vehicle positioning accuracy requirements for communication-based cooperative collision warning," *J. Intell. Transp. Syst.*, vol. 10, no. 3, pp. 131–140, 2006.
- [40] *INET Framework INET Framework*. Accessed: Jul. 3, 2019. [Online]. Available: <https://inet.omnetpp.org>
- [41] A. Kesting, M. Treiber, and D. Helbing, "Enhanced intelligent driver model to access the impact of driving strategies on traffic capacity," *Philos. Trans. Roy. Soc. A, Math., Phys. Eng. Sci.*, vol. 368, no. 1928, pp. 4585–4605, 2010.
- [42] E. Egea-Lopez, J. J. Alcaraz, J. Vales-Alonso, A. Festag, and J. Garcia-Haro, "Statistical beaconing congestion control for vehicular networks," *IEEE Trans. Veh. Technol.*, vol. 62, no. 9, pp. 4162–4181, Nov. 2013.
- [43] M. Behrisch, L. Bieker, J. Erdmann, and D. Krajzewicz, "SUMO—Simulation of urban mobility: An overview," in *Proc. SIMUL*, Oct. 2011, pp. 63–68.



**JUAN AZNAR-POVEDA** received the bachelor's and master's degrees in telecommunications engineering from the Universidad Politécnica de Cartagena, Cartagena, Spain, in 2016 and 2018, respectively, where he is currently pursuing the Ph.D. degree with the Information Technologies and Communications Department. His bachelor's degree final project was awarded Second Place in the Liberalization Telecommunications Award given by the National Association of Technical Telecommunication Engineers, in 2016, and the master's final project was awarded the Extraordinary Master Award by the Universidad Politécnica de Cartagena. His research interests include vehicular networks, deep learning, optimization algorithms, electronics, and electrochemical sensing.



**ESTEBAN EGEEA-LOPEZ** received the Telecommunications Engineering degree from the Universidad Politécnica de Valencia (UPV), Spain, in 2000, the master's degree in electronics from the University of Gavle, Sweden, in 2001, and the Ph.D. degree in telecommunications from the UPCT, in 2006. He is currently an Associate Professor with the Department of Information Technologies and Communications, UPCT. His research interests include vehicular networks and MAC protocols.



**ANTONIO-JAVIER GARCIA-SANCHEZ** received the M.S. degree in industrial engineering and Ph.D. degree from the Universidad Politécnica de Cartagena (UPCT), Spain, in 2000 and 2005, respectively. Since 2001, he has been a member of the Department of Information Technologies and Communications (DTIC), UPCT. He is currently an Associate Professor with the UPCT and the Head of the DTIC. He is the coauthor of more than 80 conference and journal articles, and forty of them indexed in the journal citation report (JCR). He has been the leader of several research EU/national/regional projects in fields of communication networks and optimization. His main research interests include wireless sensor networks (WSNs), LPWAN, streaming services, machine learning techniques, smart grid, the IoT, and health applications. He is also the inventor/coinventor of ten patents or utility models. He has been a TPC member or Chair of more than thirty international congresses or workshops. He is currently a Reviewer of several journals listed in the ISI-JCR.



**PABLO PAVON-MARIÑO** received the M.Sc. degree in telecommunication engineering from the Universidad de Vigo, Spain, in 1999, and the M.Sc. degree in mathematics and the Ph.D. degree from the Universidad Politécnica de Cartagena, in 2004 and 2010, respectively. In 2000, he joined the UPCT, Spain, where he is currently a Full Professor with the Department of Information Technologies and Communications. His research interests include the planning and optimization of communication networks.

...